

Deformation Behaviour of Pearlite in the Copper-Aluminium System

P. RODRIGUEZ, M. K. ASUNDI

Metallurgy Division, Bhabha Atomic Research Centre, Trombay, Bombay, India

The room temperature mechanical properties of eutectoidal binary aluminium bronze (Cu + 11.8 wt % Al) have been studied as a function of interlamellar spacing in the pearlite. Specimens with different lamellar spacings were produced by isothermal transformations at various sub-critical temperatures. The proportional limit, 0.2% yield strength and fracture strength were found to be inversely related to the square root of the lamellar spacing. This is in accordance with the mechanism suggested by Ansell and Lenel for deformation of two-phase alloys, according to which the criterion for macroscopic yielding is the fracture of the non-deformable phase, caused by the stress-concentration due to pile-up of dislocations at the lamellar interfaces. Metallographic evidence supporting the suggested mechanism is also presented.

1. Introduction

Strengthening by a second phase, for the same volume fraction, is determined by the size, shape and distribution of the dispersed phase. Of particular interest is the deformation behaviour of pearlitic eutectoid structures. Here, the two phases are lamellar in shape and neither of them is a matrix, since both are quasi-continuous. The relation between the morphology of such alloys and their deformation behaviour has been subjected to very little systematic study, even though interest in the subject dates back to the forties. Gensamer and his co-workers [1] were the first to investigate the relationship. Their studies on a number of pearlitic steels led to the well-known Gensamer relationship

$$\sigma = A - B \log \lambda \quad (1)$$

between the yield strength σ and the interlamellar spacing λ ; A and B are constants. Turkalo and Low [2] and Roberts *et al* [3] found that this relationship was obeyed not only in pearlitic steels but in spheroidised steels as well; in the latter case, λ becomes the interparticle spacing. In spite of this agreement with experimental results in a wide range of dispersed structures, the validity of the Gensamer relationship has been questioned. For example, Ansell and Lenel [4] have criticised the relationship as being purely empirical. (A proposed explanation for the equation is based on an assumed relationship between the rate at which dislocations are

generated and the applied stress, which assumption is not acceptable in the light of modern dislocation theory.) Ansell and Lenel have developed an alternative theory for yielding of two-phase structures which predicts that the yield strength will be inversely proportional to the square root of the interlamellar spacing.

According to Ansell and Lenel, yielding occurs in a two-phase alloy when the shear stress, due to the dislocations piled up at the interface, fractures or plastically deforms the dispersed second-phase particle. On the basis of this physical model, they have shown that the shear yield stress will be given by

$$\tau = \sqrt{\frac{\mu b F}{2\lambda}}, \quad (2)$$

where b is the Burgers vector, μ the shear modulus of the matrix, λ the interparticle spacing and F is the yield strength or fracture strength of the dispersed phase, depending on whether the second phase is deformable or not. The mechanism suggested by Ansell and Lenel will not be applicable to structures in which dislocations are able to bypass or cut through the hardening phase. Even for cases where this does not happen, say in pearlite, there has been some reluctance to accept the Ansell-Lenel theory, owing to lack of evidence for fracture of non-deformable second phase at the time of yielding [5]. Such evidence cannot be obtained in ferrous pearlite, since

cementite in the pearlite aggregate is able to deform plastically [6]. On the other hand, pearlite in the copper-aluminium system (Cu + 11.8 wt% Al) is an ideal choice to test the validity of the Ansell-Lenel mechanism. In this eutectoidal alloy, the α -phase (Cu + 9.41 wt% Al solid solution) and γ_2 -phase (Cu₂Al), form in lamellar shape; various lamellar spacings can be obtained by isothermal transformations at different temperatures [7] and the γ_2 -phase is non-deformable.

2. Experimental Procedures

The experimental alloy, aluminium bronze, of eutectoidal composition (Cu + 11.8 wt% Al) in a 500g quantity, was induction-melted in vacuum. The ingot was hot-rolled in the β -region at $\approx 800^\circ\text{C}$ to sheet of 0.5 mm thickness. Tensile specimens having $12.5 \times 3.5 \times 0.5$ mm gauge dimensions were machined out of these. The specimens were quenched from the β -region at $\approx 850^\circ\text{C}$ into a NaNO₃-KNO₃ salt bath and allowed to transform isothermally to ($\alpha + \gamma_2$) pearlite. The isothermal transformation temperatures employed and the average lamellar spacings obtained at each temperature are shown in the first two columns of table I. The temperature of the salt bath was controlled to better than $\pm 2^\circ\text{C}$ of the isothermal transformation temperature. The choice of the transformation temperatures and transformation times was based on the measurements reported by Asundi and West [7].

Tensile tests were performed in a floor model Instron Machine at a constant nominal strain rate of $6.67 \times 10^{-5} \text{ sec}^{-1}$ at room temperature (25°C). A minimum of three specimens of each lamellar spacing were tested. The specimens were metallographically polished before testing to facilitate microscopic examination after

fracture. Etching, when necessary, was carried out electrolytically in a 1% aqueous solution of chromic acid.

3. Results and Discussion

3.1. Tensile Test Results

The tensile test results are summarised in table I. The strength values and work-hardening rates reported are each the mean of at least two separate tests. As seen in the table, proportional limit, yield strength, and fracture strength increase with decreasing interlamellar spacing. All the specimens broke without any necking; thus fracture strength and UTS are the same. The ductilities, as measured by the plastic strain at the time of fracture, were very low for all the interlamellar spacings. There was a general trend for ductility to decrease with decreasing spacing, but no definite correlation could be attempted because of considerable scatter in the ductility values for the same spacing. The range of ductility values for each spacing are shown in the table. It is also seen from the table that the work-hardening behaviour is not significantly influenced by the interlamellar spacing.

The strength properties (proportional limits, 0.2% yield strengths, and fracture strengths) are plotted against $\lambda^{-1/2}$ in fig. 1, and reasonably good agreement is found with the Ansell-Lenel relationship. In fig. 2, these properties are plotted against $\log \lambda$ and from a comparison between the two figures, it is seen that the experimental results fit the semilogarithmic Gensamer relationship equally as well as the $\lambda^{-1/2}$ plot. The empirical nature of the Gensamer equation and its inadequacy in the light of modern dislocation theory have already been pointed out. On the other hand the Ansell-Lenel relationship is derived on the basis of a physical picture for the

TABLE I Tensile Test Results

| Isothermal transformation temperature $^\circ\text{C}$ | Interlamellar spacing λ , \AA | Proportional limit σ_0 , kg mm^{-2} | 0.2% yield strength | 0.5% flow stress | Fracture strength kg mm^{-2} | Plastic ductility, % | Work-hardening rates | |
|--|--|---|--|--|---------------------------------------|----------------------|---|---|
| | | | $\sigma_{0.002}$, kg mm^{-2} | $\sigma_{0.005}$, kg mm^{-2} | | | $\frac{\sigma_{0.002} - \sigma_0}{0.002}$, kg mm^{-2} | $\frac{\sigma_{0.005} - \sigma_{0.002}}{0.003}$, kg mm^{-2} |
| 555 | 14 300 | 19.8 | 36.3 | 44.1 | 51.5 | 1.60-2.50 | 8460 | 2600 |
| 552 | 10 000 | 19.6 | 35.6 | 42.0 | 49.2 | 0.54-0.88 | 7890 | 2500 |
| 540 | 5000 | 28.0 | 45.5 | 54.0 | 64.5 | 1.04-1.76 | 8880 | 2840 |
| 529 | 2850 | 30.1 | 46.3 | 59.1 | 65.8 | 0.60-0.84 | 9130 | 2820 |
| 490 | 2500 | 30.0 | 45.7 | 54.7 | 64.2 | 0.52-1.20 | 7850 | 2850 |
| 520 | 2200 | 37.5 | 53.9 | 61.3 | 67.0 | 0.32-0.94 | 8680 | 3430 |
| 503 | 2100 | 27.7 | 45.6 | 54.8 | 66.6 | 0.80-1.20 | 8950 | 3050 |
| 509 | 2000 | 29.0 | 44.1 | 53.1 | 59.3 | 0.52-0.78 | 7590 | 2990 |

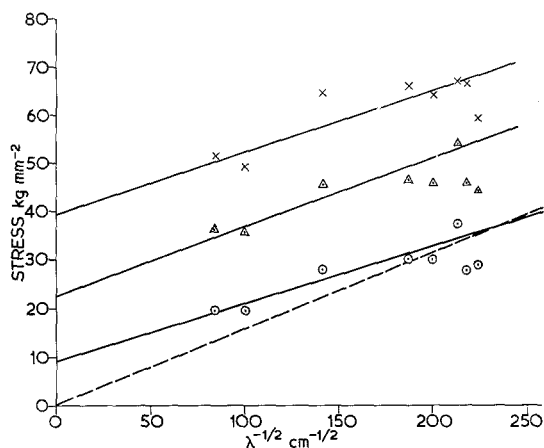


Figure 1 Strength properties plotted against $\lambda^{-1/2}$. \circ , proportional limit; \triangle , 0.2% yield strength; \times , fracture strength.

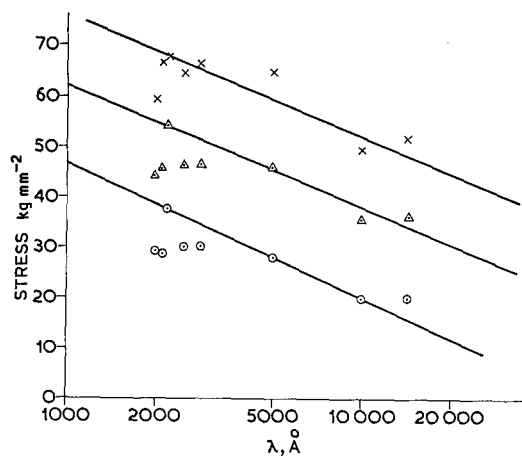


Figure 2 Strength properties plotted against $\log \lambda$. \circ , proportional limit; \triangle , 0.2% yield strength; \times , fracture strength.

deformation process. According to the theory, the criterion for macroscopic yielding of a two-phase alloy containing a non-deformable second phase is the fracture of the second phase. This fracture occurs as a result of the stress-concentration due to the pile-up of dislocations at the interface. Their calculations, which are applicable to pearlites and other structures which contain displaced particles of such a size and shape (e.g. flat plates and large spheres) that the piled-up dislocations have a large radius of curvature and so can be considered straight, lead to equation 2 for the shear yield strength (elastic limit to be

precise). The tensile elastic limit σ can be approximated as

$$\sigma = \sqrt{\frac{2\mu bF}{\lambda}} \quad (3)$$

We determined the fracture strength of the intermetallic compound Cu_2Al (γ_2) from compression tests on specimens of ≈ 5 mm diameter and ≈ 10 mm length. The compression specimens were cut and ground from cast rods. Fracture of Cu_2Al occurred within the elastic region itself and though there was considerable scatter in the fracture strength results, a maximum value of 97 kg mm^{-2} was obtained in a number of specimens. Taking a value of 100 kg mm^{-2} for F , $2.5 \times 10^{-8} \text{ cm}$ for b and 5000 kg mm^{-2} for μ , σ , the tensile elastic limit was calculated as a function of λ for the various lamellar spacings. The dashed line in fig. 1 represents this predicted variation of elastic limit with lamellar spacing. The solid lines in the figure are least-square fits with the experimental points. [The strength values for the two finest lamellar spacings, 2100 \AA ($\lambda^{-1/2} = 218$) and 2000 \AA ($\lambda^{-1/2} = 224$), were not included for obtaining the least square line. For these spacings, the strength values obtained were much lower than that for coarser spacings. These spacings were obtained by isothermal transformations at 503 and 509° C respectively and formation of some pre-eutectoidal α is known to occur at these temperatures. The lower strength values obtained in the two cases are most likely due to the formation of pre-eutectoidal α . Bearing in mind that the experimentally determined fracture strength of γ_2 could be a low figure owing to micro-defects in the cast rods, and the fracture strength of γ_2 lamellae would be expected to be somewhat different from that of bulk specimens, the agreement between the experimental values and the theoretical line is quite good.

3.2. Metallographic Studies

Fractured specimens were metallographically examined to throw light on the mechanisms of deformation and fracture. Figs. 3a and 3b show typical microstructures near the fracture area. As seen in fig. 3a fracture is both interlamellar and intralamellar in nature. The fracture path was always approximately perpendicular to the tensile axis. Separation in those lamellae that were lying normal to the tensile axis occurred at the lamellar interfaces (upper left-hand corner of fig. 3a), whereas fracture propagated in an intra-

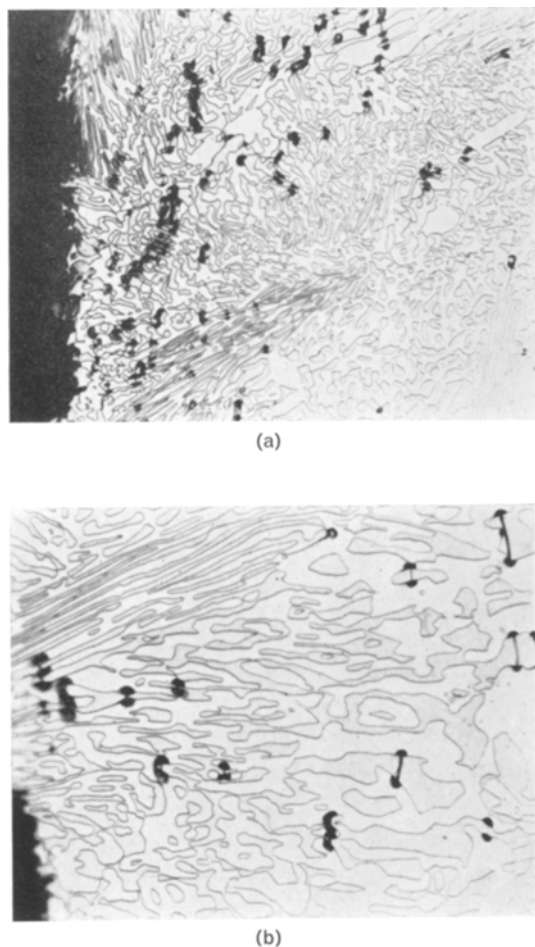


Figure 3 Typical microstructure near fracture. Electrolytic etching in 1% aqueous chromic acid (a) ($\times 293$); (b) ($\times 412$)

lamellar manner in lamellae that were lying parallel to the tensile axis and normal to the fracture path (lower left-hand corner of fig. 3b).

Another interesting observation is that cracks were prevalent in the γ_2 -phase. These can be seen in both figs. 3a and 3b and more clearly in fig. 3b. Etching seems to have preferentially attacked the phases on either side of the cracks; dumb-bells are seen in the microstructures with the cracks in the γ_2 -phase as the bar and etched region and the α -phases on either side as spheres of the dumb-bell. The density of such cracks in γ_2 is very high near the fracture, but decreases with increasing distance from the fracture region and the cracks are unobserved in regions far away from the fracture.

While these observations suggest that fracture of γ_2 -phase occurs during deformation or at the

time of ultimate failure of specimens, this is not adequate proof for the Ansell-Lenel theory. According to the Ansell-Lenel mechanism, fracture of the γ_2 -phase would have occurred at the time of macroscopic yielding itself. To test this, we metallographically examined specimens that had been given very small plastic strains (0.05 to 0.35%) and unloaded well before fracture. Cracks in γ_2 could be detected even at plastic strains as small as 0.1%. At these small strains, the frequency of such cracks was very low, but this was found to increase with strain. Another interesting observation is that cracks in γ_2 do not appear to be distributed in the entire sample. In certain regions a large number of γ_2 lamellae have fractured, whereas no cracks could be detected in other regions. This would mean that plastic deformation is localised, probably because of stress concentration, in favourable regions, and γ_2 fractures and ultimate fracture of the specimen then occurs in one of such areas.

It should be mentioned here that the cracks in γ_2 were revealed by etching only. In the as-polished condition the cracks were not visible, but slip traces in α -lamellae could be detected and most of these slip traces were observed to lie at about 45° to the tension axis. Electrolytic etching in an aqueous solution of 1% chromic acid was employed, and this revealed the cracks in γ_2 . Quite often cracks were located at the intersection of the slip traces in α - with γ_2 -lamellae. Fig. 4 is a typical microstructure of a region where cracks in γ_2 could be observed after a plastic strain of about 0.35%. The dumb-bell shapes of the etched cracks, described earlier, are seen in this figure also. According to the theory of Ansell and Lenel, fracture of the γ_2 -phase is caused by the stress due to the pile-up of dislocations at the interface (that is, there should be a pile up of dislocations in the α -phases on either side of a crack). This would then explain the preferential etching (something akin to an etch-pit attack) of the α -phase near the crack in γ_2 , leading to the dumb-bells in the microstructure.

No cracks could be observed in lamellae lying perpendicular to the tensile axis. The γ_2 -lamellae in which cracks could be observed were all more or less lying parallel to the tensile axis, and the cracks in such lamellae tended to form perpendicular to the tensile axis. This would be expected from the Ansell-Lenel mechanism. The resolved shear stress would be a maximum at 45° to the tension axis and dislocations would pile up at

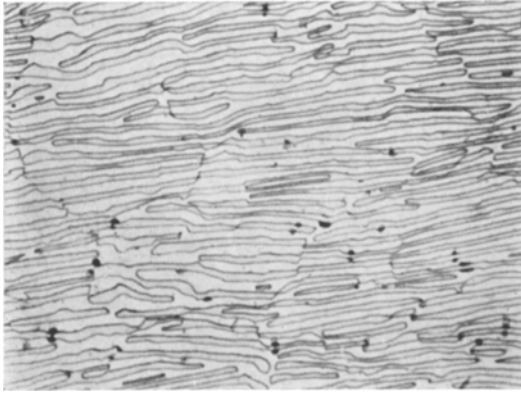


Figure 4 Microstructure of specimen given 0.35% plastic strain ($\times 97$). Etching same as fig. 3.

45° to the interfaces of lamellae lying parallel to the tension axis. The effective shear stress in γ_2 due to this pile-up, which would act at 45° to the tension axis, would have a normal component of the same magnitude but acting parallel to the tension axis, and cracks would form perpendicular to the tension axis in these lamellae. This would also explain why cracks were not observed in lamellae that were oriented normal to the tensile axis.

4. Summary

The strength properties of eutectoidal aluminium bronze varies with the interlamellar spacing in the pearlite, obeying the Ansell-Lenel mechanism of deformation in two-phase alloys which predicts an inverse relationship between strength and the square root of the interlamellar spacing. Additional evidence for the mechanism has been obtained from metallographic studies. The appearance of cracks in the hard γ_2 -phase has been observed even at plastic strains as small as 0.1%, which lends support to the view that the criterion for macroscopic yielding in the alloy is

the fracture of the non-deformable γ_2 -phase. The view that this fracture is caused by the stress-concentration due to pile-ups of dislocations at the interface is also supported by the fact that cracks in the γ_2 -phase are seen not in lamellae that are perpendicular to the tension axis but only in lamellae that lie parallel to it. Also the cracks invariably form normal to the tensile axis. Another observation which supports the hypothesis that pile-up of dislocations at the interface causes the cracks is the preferential etching into the α -phase on either side of the cracks.

Acknowledgement

This research was carried out at the Metallurgy Division of Bhabha Atomic Research Centre, Trombay, Bombay and we thank Dr V. K. Moorthy, Head, Metallurgy Division, for permission to publish this article. We acknowledge the able assistance of Mr M. Unnikrishnan in carrying out the heat-treatments and metallographic examinations and of Mr K. G. Samuel in performing the tensile tests. We are grateful to Dr V. S. Arunachalam for many stimulating discussions.

References

1. M. GENSAMER, *Trans ASM* **36** (1946) 30.
2. A. M. TURKALO and J. R. LOW, *Trans. Met. Soc. AIME* **212** (1958) 150.
3. C. S. ROBERTS, R. C. CARUTHERS, and B. C. AVERBACH, *Trans. ASM* **44** (1952) 1150.
4. G. S. ANSELL and F. V. LENEL, *Acta Met.* **8** (1960) 612.
5. R. W. K. HONEYCOMBE, "Plastic Deformation of Metals" (Edward Arnold, London, 1968) p. 185.
6. B. R. BUTCHER and H. R. PETIT, *J. Iron and Steel Inst.* **204** (1966) 469.
7. M. K. ASUNDI and D. R. F. WEST, *J. Inst. Met.* **94** (1966) 19.

Received 17 and accepted 28 November 1969.